X-Ray Diffraction Analysis to Study the Effect of Metal Loading and Calcination and Reduction Temperatures for Supported Palladium Catalysts

[1]MUHAMMAD HAMID SARWAR WATTOO*, [1]MUHAMMAD MAZHAR, [2]MUHAMMAD TUFAIL, [3]FEROZA HAMID WATTOO, [2]MAQSOOD AHMAD, [1]SYED AHMED TIRMIZI AND [4]JAVED IQBAL

[1]*Department of Chemistry, Quaid-i-Azam University, Islamabad – 45320, Pakistan.*
[2]*Ashfaq Ahmad Research Laboratories, R -Block, [2A]PINSTECH-Complex, Nilore, Islamabad, Pakistan.*
[3]*Institute of Biochemistry, University of Sindh, Jamshoro – 76080, Pakistan.*
[4]*Institute of Chemistry, University of the Punjab, Lahore – 54590, Pakistan.*

(Received 4th June 2007, revised 10th December 2007)

Summary: XRD have been used to study Pd/γ-Al_2O_3 catalysts prepared by solution impregnation method. Effect of metal loading and calcination and reduction temperatures were studied to observe active metal particles growth. On calcination, growth of tetragonal PdO was observed only at 400 and 500 °C. However, for hydrogen reduced catalysts, fine face centred cubic particles growth was observed even for 300 °C treated catalysts. Catalysts with metal loading < 2 % cannot be evaluated by their XRD spectra. In hydrogen reduced catalysts, peaks became sharpened when metal loading was increased to reasonable level. Results showed that XRD technique can be extensively used to study reduced metal particles rather to study oxidised one but to definite metal levels that can show Bragg's angle of diffraction. It has also been observed that growth of both PdO and Pd particles was increased with the elevated temperature.

Introduction

General trend in catalyst preparation is to design and synthesize active metal particles into some inert and highly porous inorganic supports [1]. In the recent years, there has been increased interest in tailoring γ-alumina impregnated palladium particles [2-6]. Supported palladium catalysts are being used in many organic transformations like Mizoraki-Heck [6], Suzuki-cross coupling [7], Stille [8], Sonogashira [8] and Hiyama cross-coupling reactions [9]. Particle size and crystal structure of these active metal palladium has a special role in all these transformations. Less attention has been given on the crystal structure and morphology of active metal particles growth under controlled calcination and reduction temperatures. By varying temperature, active metal particle growth and their size and dispersion can be tailored and more genuine correlations can be revealed.

It is now widely accepted that large particles show very small metal dispersion. This means smaller the clusters of atoms, the higher the percentage of atoms on the surface and this property makes nanoparticles very interesting in catalysis. In the present paper, we have studied the effect of metal loading and different calcination and reduction temperatures on the growth of palladium particles impregnated on γ-Al_2O_3 support by X-ray diffraction technique [10-15].

Keeping in view the findings of Monteiro *et. al.* and Zurita *et. al.*, [16, 17], we, in the present study, have selected $PdCl_2$ precursor to impregnate palladium particles on γ-alumina support by solution impregnation method. Calcination and reduction experiments were carried out at temperatures of 300, 400 and 500 °C respectively. Higher temperature was avoided due to agglomeration of small particles into large sizes. % metal loading was determined by differential pulse polarography [18-19].

Results and Discussion

We have selected γ-alumina support because it is non-reducible, thermally stable at temperature 400-500 °C, contain both tetrahedral and octahedral coordination and allows the good dispersion of active metal particles, i.e. Pd, due to its high surface area (up to 300 m^2g^{-1}) [20, 21]. Fig. 1 shows the phase transitions and surface areas of Al_2O_3 (boehmite) as a

*To whom all correspondence should be addressed.

function of temperature. % metal loading and XRD characteristics of both calcined and reduced Pd/γ-Al_2O_3 catalysts at different temperatures are given in Table-1.

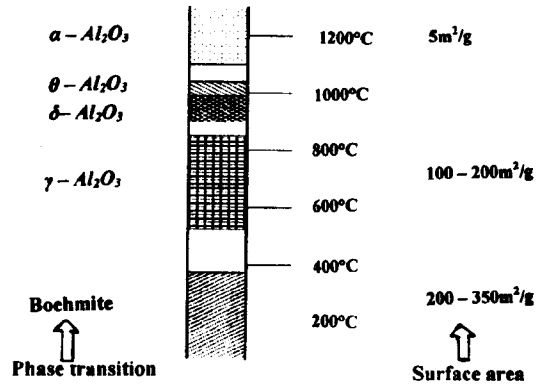

Fig. 1: Phase transitions and surface areas of Al_2O_3 (boehmite) as a function of temperature.

Table-1: % metal loading and XRD characteristics of calcined Pd/ γ-Al_2O_3 catalysts at different temperatures.

Calcined catalyst	Metal (%)	2θ	I/I.	d	Reduced Catalyst	2θ	I/I.	d
Pd-300C-2	1.6	36.935	53	2.432	Pd-300CR-2	36.935	53	2.432
		46.085	54	1.968		46.075	54	1.968
		66.765	57	1.400		66.765	57	1.400
Pd-300C-5	4.5	37.105	45	2.421	Pd-300CR-5	36.555	43	2.456
		45.825	44	1.978		39.985	58	2.253
		66.425	49	1.406		46.195	49	1.963
		--	--	--		66.455	46	1.406
Pd-300C-10	9.2	36.975	43	2.429	Pd-300CR-10	39.925	76	2.256
		45.965	40	1.973		46.395	54	1.955
		66.225	39	1.410		66.615	42	1.403
Pd-400C-2	1.6	36.905	56	2.434	Pd-400CR-2	37.225	60	2.413
		46.015	54	1.971		46.425	58	1.954
		66.435	62	1.406		66.805	66	1.399
Pd-400C-5	4.5	36.685	58	2.448	Pd-400CR-5	40.035	111	2.250
		46.045	56	1.969		46.485	72	1.952
		66.365	54	1.407		66.575	57	1.403
Pd-400C-10	9.2	36.305	40	2.472	Pd-400CR-10	4.165	115	2.243
		44.665	37	2.027		46.685	75	1.944
		67.075	34	1.394		66.775	48	1.400
Pd-500C-2	1.6	37.245	60	2.412	Pd-500CR-2	32.455	47	2.756
		46.415	60	1.955		36.835	62	2.438
		66.995	70	1.396		39.625	61	2.273
		--	--	--		45.935	65	1.974
		--	--	--		60.775	27	1.523
		--	--	--		66.875	11	1.398
Pd-500C-5	4.5	33.985	68	2.636	Pd-500CR-5	31.895	45	2.803
		37.855	59	2.375		37.985	62	2.367
		46.305	59	1.959		40.245	119	2.239
		60.525	30	1.528		46.785	84	1.940
		67.005	63	1.395		67.095	72	1.394
Pd-500C-10	9.2	33.815	71	2.648	Pd-500CR-10	31.515	37	2.836
		37.745	48	2.381		36.755	45	2.443
		46.145	43	1.965		40.225	151	2.240
		54.735	24	1.676		46.715	84	1.943
		60.475	25	1.530		67.875	54	1.380
		66.475	44	1.405		--	--	--

Fig. 2 shows that γ-Al_2O_3 consists of single phase of crystalline cubic structure (JCPDS 10-0425, ICPDS 29-63) and is not affected by a hydrogen treatment at or below 500 °C. Unterberger et al. [22] reported that hydrogen induced reduction from PdO to Pd did not exhibit promoting effect at 100 °C and further increase of temperature above 550 °C induces wetting and coalescence with γ-Al_2O_3 followed by metal-metal bonds and alloy compounds which are not desirable for effective catalytic reactions that is why we have not gone above 500 °C for both calcination and reduction steps.

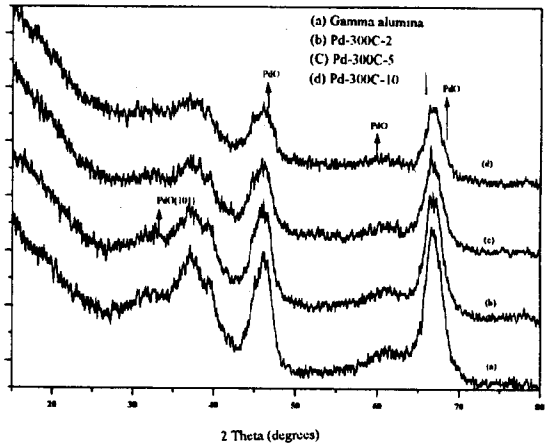

Fig. 2: γ-alumina supported monometallic Pd catalysts calcined at 300 °C.

Samples after Calcination in Air – PdO Particles

Pd oxidation is a reversible solid state reaction, $2PdO \leftrightarrow 2Pd + O_2$, with the thermodynamic parameters $\Delta H°_{1050\ K}$ = 25.7 kcal/mol and $\Delta S°_{1050\ K}$ = 22.3 cal/ (mol K). This transformation is slow since it involves diffusive process within the particle.

Figs. 2 and 3 show XRD diffraction peaks of alumina supported Pd particles calcined at 300 and 400 °C respectively. X-ray diffraction measurements using Cu $K_{\alpha 1}$ radiation do not show the presence of PdO for samples treated at lower temperatures. This may be due to the reason that very small crystallite sized particles do not give normal diffraction patterns due to lack of sufficient degree of order. It is observed (Figs. 2-4) that 1.6 % Pd loading does not show any diffraction peaks. However line broadening is observed for 4.5 % and 9.2 % Pd loading at

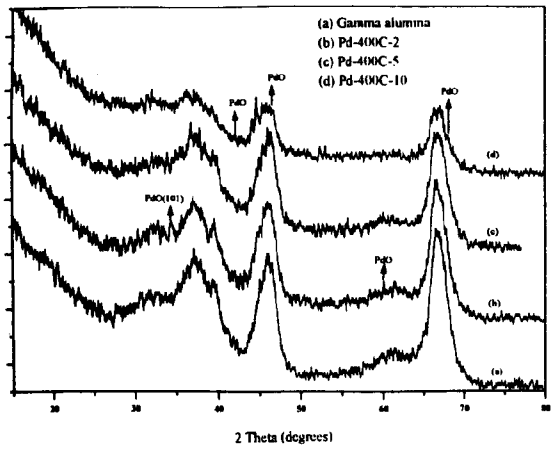

Fig. 3: γ-alumina supported monometallic Pd catalysts calcined at 400 °C.

hence diffraction peaks are observed at 2θ of 34°. This means that temperature reached was high enough to promote the oxide formation and crystallization. These crystalline patterns observed in the diffractograms are not so obvious when the catalysts are examined by the SEM. The very fine crystals detected for high temperature samples in the X-ray diffraction are not visible by SEM, even at high magnification.

Fig 4 shows XRD diffraction peaks of alumina supported Pd particles calcined at 500 °C. Again 1.6 % Pd loading does not show any diffraction peaks. However a sharp PdO characteristic peak is observed at 2θ of 33.985° for 4.5 % Pd catalyst and at 2θ of 33.815° for 9.2 % Pd catalyst. This peak becomes more intense and sharp when Pd loading exceeds to 9.2 %. The resulting pattern was compared with ICDD files (43-1024 and 46-1043 for tetragonal PdO). Tetragonal PdO [a = b = 3.043A° (0.304 nm), c = 5.337A° (0.534 nm)] was identified by its XRD peaks at 2θ of 33.8° (101) plane and 54.7° (112) plane.

calcination temperature of 300 and 400 °C respectively. This is in evidence that for very small particles, X-ray reflection occurs over a small range of angles and line becomes broadened. Line broadening is detectable when particle size is less than 0.1 μm because X-ray diffraction is insensitive to study changes in particle sizes between 0.1 μm and about 10 μm. This indicates that at low temperatures and at Pd loading < 2 %, the PdO crystallites are too small to be observed by XRD.

The particle size determined by XRD analysis for PdO (101) for 4.5 % and 9.2 % loading is 0.16 nm. In contrast, the SEM images show particles that could be agglomerates of small particles or crystallites. The size of the agglomerates could be estimated by SEM, but crystallite size is more difficult to determine unless it is well dispersed. Hence, the disparity between XRD and SEM may account for that XRD measures the average crystallite size and in the SEM images the size of the particles clearly observed.

At 400 °C, slight appearance of overlapping peak at 2θ of 46° for Pd loading 9.2 % is observed, indicates the first appearance of metallic Pd (111) and Pd (200) phases, which are then oxidized to form PdO in the presence of air at 500 °C (Fig. 4) and

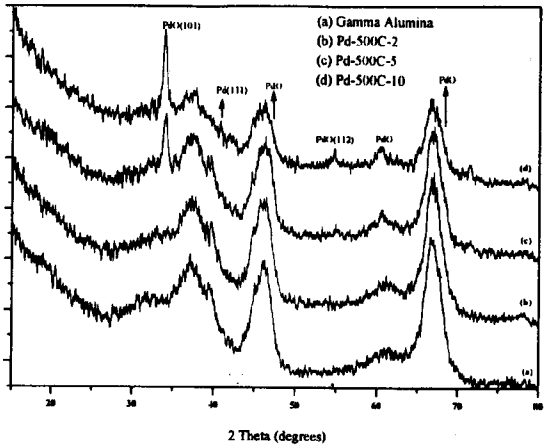

Fig. 4: γ-alumina supported monometallic Pd catalysts calcined at 500 °C.

When temperature is increased up to 500°C, four new signals appeared for 4.5 % and 9.2 % Pd loading which can also be attributed to the tetragonal phase of PdO (JCPDS 431024; a peak at 2θ of 33.8° and other signals at 2θ of 41.9°, 54.7° and 60°. Peak broadening for 4.5 % and 9.2 % Pd loading at 2θ of 46° indicates the first appearance of metallic Pd (111) and Pd (200) faces at calcination of 300, 400, 500°C. However, the crystal size of metallic Pd seems to be extraordinary lower for calcined samples when compared with the reduced ones (Fig 5). The characteristic peak for PdO at 2θ of 34° varies in sharpness and intensity possibly due to the differences in particle size and amount of Pd in the crystal phase. Viswanathamurthi et al.[2] reported

that in the absence of γ-alumina support, characteristic diffraction peaks of PdO appear at 2θ of 33.8°, 40.2°, 41.8°, 46.5°, 54.0°, 60.0° and 68.1° at the calcination temperature of 500 °C. Owing to the overlapping with alumina peaks (ICDD file no. 10-0425), the other main peaks of PdO (41.948° and 60.207°) could not be used for structure identification but they show their presence by overlapping and broadening of γ-alumina peaks. PdO crystallites of calcined catalysts increased in size with the increase of Pd loading and PdO diffraction lines become stronger with the increase of Pd loading. By increasing temperature the loaded Pd is agglomerated to form PdO which is then detected by XRD.

Samples after Reduction with Hydrogen-Pd particles

Lyubovsky et.al. [10] described from their TGA data that it must take approximately 10 min at 797 °C for complete transformation from, $PdO \rightarrow Pd$, without involving hydrogen reduction. The palladium metal particle size increases with increasing temperature and the crystallites acquired more regular shapes at 800 °C. In addition to triangular particles at higher temperatures (800 °C), other shapes including some hexagonal particles also appear.

At higher temperature, decomposition of PdO leads to the formation of a metallic Pd surface. This appears to cause a large increase in particle mobility over the alumina support, leading to increased agglomeration and low-index Pd surfaces are formed. The reported particles [10] were much bigger in size than usually required for supported catalysts. Moreover, high temperature reduction changes highly porous γ-Al_2O_3 support to less porous δ-Al_2O_3, θ-Al_2O_3 and α-Al_2O_3 respectively (Fig. 1). The active metal particles become less dispersed and sintering of Pd with Al might be expected to form alloy. The only best way for catalyst reduction at low temperature is by hydrogen treatment.

Fig. 5 shows the presence of a signal at 2θ of 40.0° which is assigned to Pd metal (JCPDS 5-681) and can be assessed from the diffractogram at 400°C. The resulting pattern was also compared with ICDD files (5-0681 and 40-1024 for metallic Pd). Cubic Pd (a = 3.8898A° and a = 0.389 nm) was identified by its XRD peaks at 2θ of 40.115° (111) plane. In fact, only the most intense peaks emerging

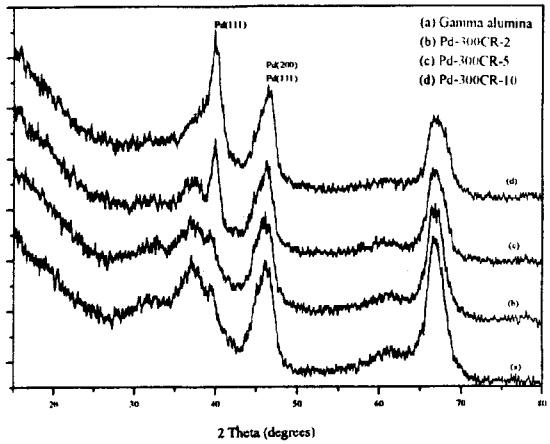

Fig. 5: γ-alumina supported monometallic Pd catalysts reduced at 300 °C.

from the alumina background were used as a reference. The line positions were checked by using an internal standard (Si monocrystal).

Owing to the overlapping with alumina peaks (ICDD file no. 10-0425), the other main peak of metallic Pd (46°) could not be used for structure identification, however, it indicates the broadening of alumina peak by overlapping. At reduction temperatures of 400°C and 500°C, these diffraction peaks are slightly distinguishable from γ-alumina support peaks. The catalyst particle size also increases during reduction due to the high mobility of βPdH. Metallic Pd has major diffraction peaks at 2θ of 40° (111) and 46° (200) at temperatures of 300°C 400°C and 500°C for Pd loading higher than 1.6 %. However, no such diffraction peaks were observed at these reduction temperatures for Pd loading < 1.6 %, indicating that Pd was highly dispersed. However, at 500°C, a slight appearance or tailing of peak at 2θ of 45° (111) is visible. Peaks due to metallic Pd (for example, Pd (111) and (200) around 2θ of 40° and 47°, respectively) become sharper and sharper with an increase in the activation temperature, indicating that the Pd metal particles rapidly grow with heating.

SEM images of some selected calcined and reduced monometallic Pd/γ-Al_2O_3 catalysts are given in Fig. 8. The size of the Pd metal particles determined from the Pd (111), using Scherer equation, was 0.04 to 1.06 nm. SEM images show that Pd particles are uniform (1-2 nm) in size and are homogeneously dispersed into the alumina support.

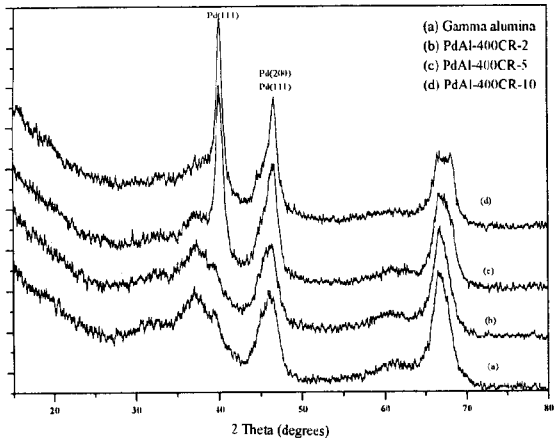

Fig. 6: γ-alumina supported monometallic Pd catalysts reduced at 400 °C.

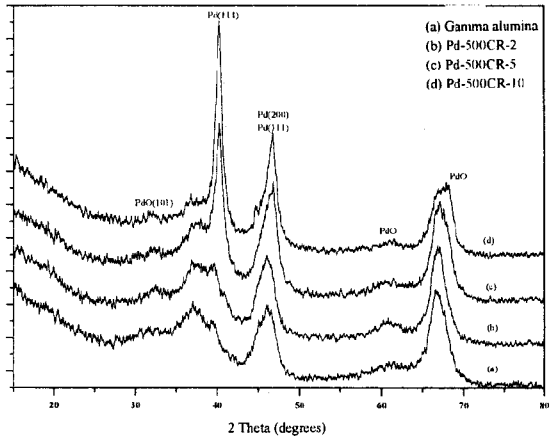

Fig. 7: γ-alumina supported monometallic Pd catalysts reduced at 500 °C.

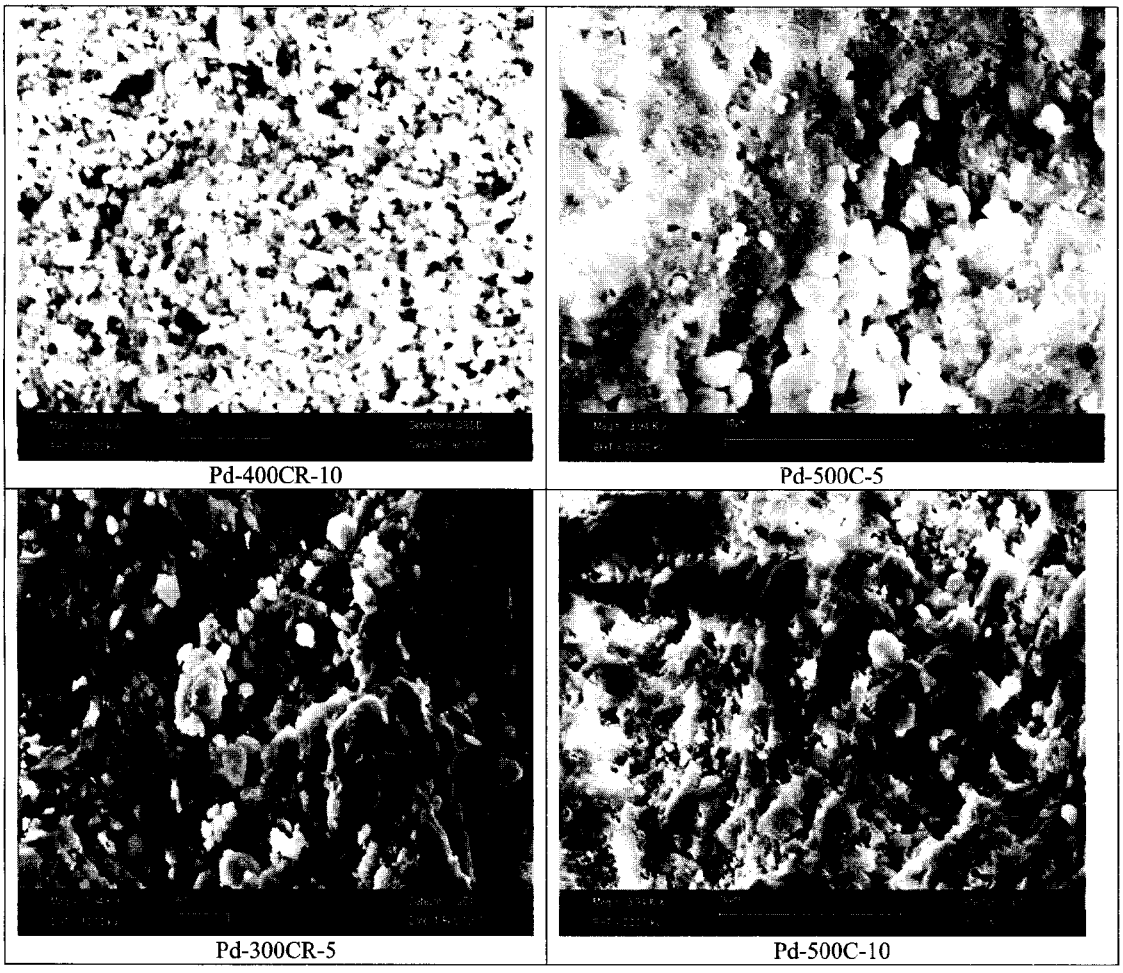

Fig. 8: SEM images of some selected calcined and reduced monometallic Pd/γ-Al_2O_3 catalysts.

Elevated hydrogen reduction temperature activated alumina supported Pd catalysts shows somewhat smaller Pd particles than that activated at high temperature without hydrogen treatment [10]. This is probably due to the fact that amorphous structure of Pd particles is densified by heating at high temperature.

SEM observations are less consistent with the XRD results. The difference in particle size between XRD and SEM for catalysts activated at 500 °C is higher. It has been suggested [15, 16] that at high temperature reduction, γ-alumina support gains considerable lewis acidity and introduction of Pd to alumina reduces acidity of the support. This gives super embeddings of the active metal palladium particles on the γ-alumina support for its various catalytic reactions.

Experimental

Materials

Catalyst support grade, highly porous γ-alumina pellets (BET = 250 m^2/g, Alfa Aesar® - Germany) were used to impregnate palladium metal particles. Palladium chloride was purchased from Degussa AG – Germany and was used as received. All other reagents used were of AR purity. Freshly prepared deionised water was used throughout this study.

Support Pre-treatment

Small spheres of γ-alumina were machine grinded and then were sieved with US standard sieves to get 40-60 mesh granules. These granules were washed with 0.2M HCl followed by deionised water and dried in an oven overnight at 80 °C. To achieve mechanical stability, granules were baked in a muffle furnace in an air flow using the ramp rate 2 °C/mint and soaked at 400 °C for 4 hours. Before use, the support was heated under vacuum of 1×10^{-6} mbar for 4 hours at 200 °C to clean it from lose dust particles and to get maximum pore opening.

Palladium Particles Impregnation

It is clear that smaller metal particles are obtained when $PdCl_2$ is used as palladium precursor [17]. Required weight of $PdCl_2$ was dissolved in minimum amount of 0.2M HCl solution in a beaker continuous stirring and heating at 80 °C till complete dissolution and made the volume to mark with deionised water to get the desired precursor solution for impregnation. Mixed the support and impregnating solution in a pear shaped flask, rotated at 40 rpm for 6 hours in a rotary evaporator (SteroGlass model-202) under positive pressure and using water bath at 80 °C. Magnetic stirring was avoided due to crushing of support material by the magnetic bar stirring. Excess water was eliminated under vacuum. The material was then dried overnight in an oven at 80 °C. Abrupt high temperature for drying was avoided to care for leaching out of palladium from the micropores with the out going bubbles due to surface tension phenomenon.

Calcination and Reduction

Material was calcined in air flow at 300, 400 and 500 °C respectively in a muffle furnace using ramp rate of 2 °C/mint and soaked at respective temperature for 4 hours. Same procedure was used for reduction of these catalysts in a hydrogen flow using the tube furnace. Both calcined and reduced catalysts were immediately transferred to airtight bottles for various analyses.

Percentage Metal Loading

A polarographic analyzer (Metrohm 746 VA) equipped with droping mercury electrode (Ag/AgCl/3KCl 3M) and auxiliary Pt electrode was used for the determination of percentage palladium loadings on the γ-alumina support. Differential pulse polarography with standard addition method was used to record the polarograms. NH_3/NH_4Cl solution of pH = 9.6 was used as a supporting electrode and $U_{1/2}$ was 825 mV. Hydrofluoric acid (40 %) and hydrochloric acid (37 %) were used in the digestion procedure.

X-Ray Powder Diffraction (XRD)

All the analysis were performed in a XPERT-PRO diffractometer using the Cu $K_{\alpha 1}$ radiation (λ=0.15406 nm) as a source (current intensity, 30 mA; voltage, 40 kV). Goniometer used was PW3050/60 (Theta/ 2Theta); Minimum step size 2Theta:0.001; Minimum step size Omega: 0.001. The catalyst sample (40 mg) was gently spread on a flat sample holder but care was taken to put the entire

sample under the X-ray beam of the apparatus. A 15 – 80° range of 2θ was investigated, the diffraction angle being increased by step of 0.02° every 5 seconds. XRD pattern were compared to ICDD and JCPDS files. The crystalline size was estimated using the Scherrer equation [18, 19].

$$D_{hkl} = \frac{K \lambda}{B \cos (\theta)}$$

Where D is the mean diameter of the palladium metal particles, K is 0.94, λ is the wavelength of Cu $K_{\alpha 1}$= 0.1540 nm, B is angular width (full width at half maximum-FWHM) of the X-ray diffraction peak at the diffraction angle 2θ (Bragg's angle of the peak).

Scanning Electron Microscopy (SEM

SEM was carried in a secondary electron emission mode operating at 20kV. The samples were mounted on the circular discs using silver in methyl isobutyl ketone solution supplied by Agar Scientific Ltd. Essex, UK.

Conclusion

Different sized palladium particles can be grown on alumina using different calcination and reduction temperatures. XRD cannot be used for identification of small sized metal particles formed on alumina at loading below 2 %. Due to the apparently small size of the metal particles and close values of inter-planar distances responsible for the strongest XRD reflexes in the crystal lattices of Pd. By the only using controlled oxidation and reduction temperature, different sized Pd particles can be tailored. XRD pattern for metallic Pd at low temperature i.e. 300 °C has peaks at positions very similar to γ-alumina (Pd, 2θ of 40.1° and 46.7°; γ-alumina, 2θ of 36.5°, 39.5°, 46° and 67°). This makes unequal identification of metallic Pd in the presence of alumina difficult at lower metal loadings and lower calcination and reduction temperature. These results provide guidelines for future tailoring of modern catalysts.

Acknowledgements

This paper is the findings of research project titled Effect of Temperature Treatment, Precursor Solution and Promoter on the Growth of Alumina Supported Palladium Particles. The authors acknowledge the joint support of Department of Chemistry, Quaid-i-Azam University, Islamabad and PAEC–Islamabad, for providing necessary laboratory facilities.

References

1. T. Alexis Bell, *Science* **299**, 1688 (2003).
2. P. Viswanathamurthi, N. Bhattarai, H. Y. Kim, D. I. Cha and D. R. Lee, *Mater. Lett.*, **58**, 3368 (2004).
3. A. K. Datye, J. Bravo, T. R. Nelson, P. Atanasova, M. Lyubovsky and L. Pfefferle, *Appl. Catal. A.*, **198**, 179 (2000).
4. C. F. Cullis and J. G. Firth, Detection and measurement of Hazardous Gases, Heinemann, London, 1981.
5. M. P. Dare-Edwards, J. B. Goodenough, A. Hamnett and A. Katty, *Mater. Res. Bull.*, **19**, 435 (1984).
6. M. T. Reetz and E. Westermann, *Angew. Chem., Int. Ed. Engl.*, **39**, 165 (2000).
7. A. Suzuki, *J. Organomet Chem.* **576**, 147 (1999).
8. B. M. Choudary, S. Madhi, N. S. Chowdari, M. L. Kantam and B. Sreedhar, *J. Am. Chem. Soc.*, **124**, 14127 (2002).
9. L. D. Pachon, M. B. Thathagar, F. Hartl and G. Rothenberg, *Phys. Chem. Chem. Phys.*, **8**, 151 (2006).
10. M. Lyubovsky, L. Pfefferle, A. Datye, J. Bravo and T. Nelson, *J. Catal.*, **187**, 275 (1999).
11. K. Persson, P. O. Thevenin, K. Jansson, J. Agrell, S. G. Järås and L. J. Pettersson, *Appl. Catal.*, A **249**, 165 (2003).
12. M. C. Greca, C. Moraes, M. R. Morelli and A. M. Segadães, *Appl. Catal.*, A **179**, 87 (1999).
13. M. C. Greca, C. Moraes and A. M. Segadães, *Appl. Catal.*, A **216**, 267 (2001).
14. D. H. Kim, S. I. Woo and O. B. Yang, *Appl. Catal.*, B **26**, 285 (2000).
15. M. Skotak, D. Łomot and Z. Karpiński, *Appl. Catal.*, A **229**, 103 (2002).
16. R. S. Monteiro, L. C. Dieguez and M. Schmal, *Catal. Today*, **65**, 77 (2001).
17. M. J. P. Zurita, M. Cifarelli, M. L. Cubeiro, J. Alvarez, M. Goldwasser, E. Pietri, L. Garcia, A. Abouais and J. F. Lamonier, *J. Mol. Catal.*, A **206**, 339 (2003).
18. S. Liu, K. Takahashi and M. Ayabe, *Catal. Today*, **87**, 247 (2003).

19. S. Liu, K. Takahashi, K. Uematsu and M. *Ayabe, Appl. Catal.*, A **277**, 265 (2004).
20. H. S. Potdar, K. Jun, J. W. Bae, S. M. Kim and Y. J. Lee, *Appl. Catal.*, A **321**, 109 (2007).
21. M. Digne, P. Sautet, P. Raybaud, P. Euzen and H. Toulhoat, *J. Catal.*, **226**, 54 (2004).
22. W. Unterberger, B. Jenewein, B. Klotzer, S. Penner, W. Reichl, G. Rupprechter, D. Wang, R. Schlögl and K. Hayek, *React. Kinet. Catal. Lett.*, **87**, 215 (2006).